Histol Histopathol (2024) 39: 483-496

Histology and Histopathology
From Cell Biology to Tissue Engineering

ORIGINAL ARTICLE Open Access

microRNA-105-5p protects against chondrocyte injury, extracellular matrix degradation, and osteoarthritis progression by targeting SPARCL1

Dong Jiang, Shigao Cheng, Pengcheng Kang, Tengfei Li, Xun Li, Jiongzhe Xiao and Lian Ren
Department of Orthopedic Surgery, Loudi Central Hospital, Loudi, Hunan, PR China

Summary. Objective. Both microRNA (miR)-105-5p and SPARCL1 were discovered to be differentially expressed in osteoarthritis (OA), but their roles and exact mechanisms have not been entirely elaborated. This paper sets out to probe the impact of miR-105-5p/SPARCL1 on chondrocyte injury, extracellular matrix degradation, and osteoarthritis progression.

Methods. C28/I2 cells were stimulated with IL-1β to construct an *in vitro* OA model. C28/I2 cells were transfected with sh-SPARCL1, oe-SPARCL1, or miR-105-5p mimic before IL-1β induction. CCK-8 assay, flow cytometry, and ELISA were adopted to assess cell viability, apoptosis, and inflammatory factor expression, respectively. The binding relationship of miR-105-5p to SPARCL1 was assessed using dual-luciferase reporter assay. After an OA rat model was established, rats underwent intra-articular injection with ago-miR-105-5p. TUNEL was applied to determine cell apoptosis *in vivo*. mRNA and protein levels were measured by qRT-PCR and western blot, respectively, *in vitro* and *in vivo*.

Results. IL-1β treatment diminished miR-105-5p expression and augmented SPARCL1 expression in C28/I2 cells. miR-105-5p decreased SPARCL1 expression by targeting SPARCL1. miR-105-5p overexpression or SPARCL1 silencing prominently reversed the decrease in viability and the promotion of inflammatory factor production, cartilage matrix degradation, and apoptosis in IL-1β-stimulated C28/I2 cells. Furthermore, upregulation of SPARCL1 nullified the influence of miR-105-5p overexpression on viability, apoptosis, inflammation, and cartilage matrix degradation in IL-1β-stimulated C28/I2 cells. miR-105-5p overexpression ameliorated knee cartilage tissue injury in OA rats.

Conclusion. Conclusively, miR-105-5p exerted suppressive effects on chondrocyte injury, extracellular matrix degradation, and OA progression by targeting SPARCL1.

Key words: Chondrocyte injury, Extracellular matrix degradation, Inflammatory factors, microRNA-105-5p, Osteoarthritis, SPARCL1

Corresponding Author: Lian Ren, Department of Orthopedic Surgery, Loudi Central Hospital, No. 51, Changqing Mid Street, Louxing District, Loudi, Hunan 417000, PR China. e-mail: renlian198311@163.com
www.hh.um.es. DOI: 10.14670/HH-18-654

Introduction

Osteoarthritis (OA), a prevalent disease of degenerative joint cartilage, which correlates to hypertrophic alteration, inflammation of the synovium, sclerosis of the subchondral bone, and narrowing of the joint space (Jena et al., 2021). This disease afflicts more than 300 million individuals throughout the world, and its morbidity is growing in China and the world (Disease et al., 2018; Delplace et al., 2021; Liu et al., 2022). The pathogenesis of OA is related to overweight, aging, sex, joint injury, and genetics (Chen et al., 2017; Wang and He, 2018). Moreover, OA is a prominent contributor to functional impairment and disability with substantial therapeutic expenses and socioeconomic load (Hermann et al., 2018), which calls for research on OA. As reported, chondrocytes are the sole cells of articular cartilage, which assume a pivotal function in OA pathological development through cytokine creation and cell apoptosis (Ding et al., 2019). It has been indicated that inflammation and apoptosis of chondrocytes are involved in OA pathogenesis (Feng et al., 2021). Chondrocyte apoptosis is followed by such resident cell loss in articular cartilage, leading to extracellular matrix (ECM) damage and the onset of cartilage injury (Huang et al., 2017). For that reason, mitigating inflammation, apoptosis, and injury of chondrocytes and ECM degradation may be potential targets for the treatment of patients with OA.

Secreted protein, acidic and rich in cysteine

(SPARC) family proteins are a group of proteins that orchestrate cell metastasis, proliferation, growth factor signaling, and adhesion to influence the ECM and intercellular interactions, thus participating in tissue repair and development (Chen et al., 2020). SPARC-like 1 (SPARCL1) is a secretory glycoprotein that is a member of the SPARC family of the matricellular protein (Gagliardi et al., 2017). SPARCL1 has been displayed to be engaged in the progression of various cancers, including cervical, colorectal, and ovarian cancers (Ma et al., 2018; Zhang et al., 2021, 2022). In addition, Brophy et al. also elucidated that SPARCL1 was considerably upregulated in the OA meniscus (Brophy et al., 2018). Nevertheless, there are no functional investigations of the influence of SPARCL1 on OA. As reported, microRNAs (miRNAs/miRs) govern the expression of numerous genes and thus regulate normal articular function and preserve homeostasis, including secretion of inflammatory cytokines, ECM modulation, and chondrogenesis (Endisha et al., 2021). Reportedly, miRNAs are considered to be circulating biomarkers of OA, and numerous miRNAs play a role in modulating chondrocytes through apoptosis, senescence, and pathways (Swingler et al., 2019). For instance, miR-186-5p inhibition reduced apoptosis and inflammatory injury and enhanced viability in OA by modulating MAPK1 (Li et al., 2021). Overexpression of miR-140-5p facilitated chondrocyte proliferation and diminished inflammatory response and apoptosis through high mobility group box 1 in OA (Wang et al., 2020). A preceding publication illustrated that OA patients had downregulated miR-105 expression (Ji et al., 2016). Likewise, Weng et al. uncovered that hsa-miR-105-5p expression was low in the plasma of patients with knee OA (Weng et al., 2020). Of note, the bioinformatics prediction in our research revealed that binding sites existed between microRNA (miRNA/miR)-105-5p and SPARCL1.

Therefore, we assumed that miR-105-5p might influence the process of OA by manipulating SPARCL1. This study ascertained the influence of the miR-105-5p/SPARCL1 axis on chondrocyte injury, ECM degradation, and OA progression through western blot detection of MMP13, Collagen II, ADAMTS-5, and Aggrecan expression, CCK-8, flow cytometry, HE staining, and TUNEL staining.

Materials and methods

Bioinformatics analysis

The OA-related gene expression microarray was searched in the Gene Expression Omnibus (https://www.ncbi.nlm.nih.gov/geo/) with OA as the keyword, and the GSE98918 microarray was retrieved and attained, which includes mRNA expression profiles of 12 patients with OA and 12 patients without OA (who underwent partial meniscectomy under arthroscopy) (Qiu et al., 2021). SangerBox software was employed to conduct limma test of OA and non-OA tissue samples. Differential genes were screened with |logFC| >1 and Adjust P value <0.05 as the threshold. Finally, a volcano map was plotted to present the screened differentially expressed genes.

The miRNAs binding to the screened mRNA were predicted by miRDB (http://www.mirdb.org/mirdb/index.html), Targetscan (https://www.targetscan.org), and Starbase (https://starbase.sysu.edu.cn/index.php) databases (Lin et al., 2022). A Venn diagram was drawn using Venny2.1 (https://bioinfogp.cnb.csic.es/tools/venny/) to attain the intersection of miRNAs screened by the above three databases.

Cell culture

Human chondrocyte C28/I2 cells (American Type Culture Collection, Manassas, VA, USA) are adherent cells with irregular spindle-shaped cell morphology. They were cultured in Dulbecco's Modified Eagle Medium (Gibco, Carlsbad, California, USA) encompassing 10% fetal bovine serum at 37°C with 5% CO_2. Then, C28/I2 cells were processed for 24h with 10 ng/mL interleukin (IL)-1β (200-01B, Peprotech, Rocky Hill, NJ, USA) at 37°C to mimic OA and induce inflammation (Fan et al., 2021).

Cell transfection and grouping

miR-105-5p-mimic, SPARCL1 silencing plasmids [short hairpin RNA (sh)-SPARCL1], SPARCL1 overexpression plasmid (oe-SPARCL1), and negative controls (NCs, mimic-NC, sh-NC, and oe-NC) were attained from GenePharma (Shanghai, China). The used shRNA sequences were as follows: sh-SPARCL1-1-sense sequence (SS), GGACAGTGATGGTCACTTA; sh-SPARCL1-1-antisense sequence (AS), TAAGTG ACCATCACTGTCC; sh-SPARCL1-2-SS, GACAGTG ATGGTCACTTAA; sh-SPARCL1-2-AS, TTAAGTG ACCATCACTGTC; sh-SPARCL1-3-SS, CATCAGT ACTAAAGTCAAA; sh-SPARCL1-3-AS, TTTGAC TTTAGTACTGATG. Cells were seeded onto 6-well plates (2×10^5 cells/well) 24h prior to transfection and transiently transfected using Lipofectamine 2000 (11668019, Thermo Fisher Scientific Inc., Waltham, MA, USA) as per the manufacturer's protocols, with follow-up experiments conducted after 48-h transfection (Othumpangat and Noti, 2023). The transfection dose of RNA plasmid, mimic, and inhibitor was 2 μg, 50 nM, and 100 nM, respectively.

C28/I2 cells were randomly classified into eight groups: the control, IL-1β (cells received IL-1β stimulation), miR-105-5p-mimic (cells received miR-105-5p-mimic transfection and IL-1β stimulation), mimic-NC (cells received mimic-NC transfection and IL-1β stimulation), sh-SPARCL1 (cells received sh-SPARCL1 transfection and IL-1β stimulation), sh-NC (cells received sh-NC transfection and IL-1β stimulation), miR-105-5p-mimic + oe-SPARCL1 (cells

received miR-105-5p-mimic + oe-SPARCL1 trans fection and IL-1β stimulation), and miR-105-5p-mimic + oe-NC (cells received miR-105-5p-mimic + oe-NC transfection and IL-1β stimulation) groups.

Quantitative real-time polymerase chain reaction (qRT-PCR)

TRIZOL (Invitrogen, Carlsbad, CA, USA) was employed to isolate total RNA, followed by reverse transcription as per the protocols of the Reverse Transcription Kit (Takara, Shiga, Japan). Gene expression was evaluated using a LightCycler 480 (Roche Diagnostics, Indianapolis, IN, USA) fluorescent quantitative PCR instrument with reaction conditions in accordance with the operating instructions of the fluorescent quantitative PCR kit (SYBR Green Mix, Roche Diagnostics). The thermal cycling parameters were as follows: 95°C for 10 s, 42 cycles of 95°C for 5 s, 60°C for 10 s, and 72°C for 10 s, and final extension at 72°C for 5 min. Three replicates were set up for each quantitative PCR reaction. Glyceraldehyde-3-phosphate dehydrogenase (GAPDH) or U6 was chosen as the internal reference with the $2^{-\Delta\Delta Ct}$ method for data analysis (Zhou et al., 2021). The amplification primers are detailed in Table 1.

Western blot

Protein samples were harvested by lysing the cells or tissues using Radio-Immunoprecipitation assay lysis solution (P0013B, Beyotime, Shanghai, China). Following protein concentration estimation using the bicinchoninic acid kit (P0010, Beyotime), the corresponding volume of protein was denatured by mixing with the loading buffer (P0015, Beyotime) and then heating for 3 min in a boiling water bath. Electrophoresis was performed at 80 V for 30 min and then switched to 120 V for 1-2h after bromophenol blue entered the separation gel. The transfer was carried out in an ice bath with a current of 300 mA for 60 min. Thereafter, the membranes were rinsed in the washing solution for 1-2 min and then blocked in the blocking solution for 60 min at room temperature or overnight at 4°C. The membranes were probed with primary antibodies against GAPDH (5174S, 1:1000, Cell Signaling Technologies, Beverly, MA, USA), SPARCL1 (ab255597, 1:1000, rabbit anti-human, Abcam,

Table 1. Primer sequences.

Name of primer	Sequences(5'-3')	Product size (bp)	Annealing (°C)	
miR-105-5p-F(homo) miR-105-5p-R(homo)	GGCAGGTCAAATGCTCAGAC CTCAACTGGTGTCGTGGA	59	60	
miR-105-5p-F(Rat) miR-105-5p-R(Rat)	TCGCAAGTGCTCAGATGT TGTCGTGGAGTCGGC	64	56	
SPARCL1-F(homo) SPARCL1-R(homo)	GCCTGGAGAGCACCAAGAGGCC ATGGTCCCCAGCCAAAAGCCTC	517	61	> NM_004684.6
SPARCL1-F(Rat) SPARCL1-R(Rat)	ACAACCAAGGGGCCAAGAAA ACAGTGGGGTTTTCCGTGTT	152	55	> NM_012946.2
U6-F(homo) U6-R(homo)	CTCGCTTCGGCAGCACA AACGCTTCACGAA TTTGCGT	61	55	
U6-F(Rat) U6-R(Rat)	TGGCATTGGCAGTACATATAAGA ATTTGCAGGTCACTCTTGCAC	78	58	
TNF-α-F(homo) TNF-α-R(homo)	CTGGGCAGGTCTACTTTGGG CTGGAGGCCCCAGTTTGAAT	272	55	> NM_000594.4
TNF-α-F(Rat) TNF-α-R(Rat)	GGCTTTCGGAACTCACTGGA GGGAACAGTCTGGGAAGCTC	164	55	> NM_012675.3
IL-6-F(homo) IL-6-R(homo)	TCCACAATACCCCCAGGAGA CAGCTCTGGCTTGTTCCTCA	346	54	> NM_001371096.1
IL-6-F(Rat) IL-6-R(Rat)	CACTTCACAAGTCGGAGGCT TCTGACAGTGCATCATCGCT	114	54	>NM_012589.2
IL-8-F(homo) IL-8-R(homo)	ATGACTTCCAAGCTGGCCGTGGCT TCTCAGCCCTCTTCAAAAACTTCTC	292	63	> NM_000584.4
CXCL1-F(Rat) CXCL1-R(Rat)	TGCACCCAAACCGAAGTCAT ACGCCATCGGTGCAATCTAT	149	59	> NM_030845.2
GAPDH-F(homo) GAPDH-R(homo)	AATGGGCAGCCGTTAGGAAA GCGCCCAATACGACCAAATC	168	54	> NM_001256799.3
GAPDH-F(Rat) GAPDH-R(Rat)	GCATCTTCTTGTGCAGTGCC GATGGTGATGGGTTTCCCGT	262	55	> NM_017008.4

F, forward; R, reverse.

Cambridge, UK), matrix metalloproteinase (MMP) 13 (ab39012, 1:4000, rabbit anti-human, Abcam), Collagen II (ab34712, 1:1000, rabbit anti-human, Abcam), A Disintegrin and Metalloproteinase with Thrombo-Spondin motifs (ADAMTS-5, ab41037, 1:200, rabbit anti-human, Abcam), Aggrecan (ab3778, 1:1000, mouse anti-human, Abcam), B cell lymphoma-2 (Bcl-2, ab32124, 1:1000, rabbit anti-human, Abcam), caspase-3 (ab184787, 1:2000, rabbit anti-human, Abcam), and Bcl-2-associated X (Bax, ab182733,1:2000, rabbit anti-human, Abcam) for 1h at room temperature on a shaker, and washed 3×10 min with washing solution. Subsequently, the membranes were probed with the secondary antibody (horseradish peroxidase-labeled goat anti-rabbit/mouse Immunoglobulin G, 1:5000, Abcam) for 1h at room temperature. Detection was conducted using a chemiluminescence imaging system (Bio-Rad, Hercules, CA, USA) after development of the membranes (Liu and Luo, 2019).

Dual-luciferase reporter assay

Binding sites between miR-105-5p and SPARCL1 were predicted by the Starbase website. Based on the predicted results, wild-type (WT) and mutant (MUT) sequences of the binding sites (WT-SPARCL1 and MUT-SPARCL1) were designed, synthesized, and inserted into the luciferase reporter gene vector pGL3-Promoter (Promega, Madison, WI, USA). Next, these vectors were respectively co-transfected with miR-105-5p-mimic (30 nM) or mimic-NC (30 nM) into HEK293T cells (CL-0005, Procell, Wuhan, China). Subsequent to transfection, Firefly and Renilla (the internal reference) luciferase activities were examined, and the ratio of Firefly luciferase activity to Renilla luciferase activity was the relative activity of luciferase. Luciferase activity was measured using a fluorescence detector (Promega) (Liu and Luo, 2019).

Cell counting kit (CCK)-8 assay

After C28/I2 cells were processed with IL-1β or stimulated for 24h with IL-1β after transfection, cell viability was assessed by CCK-8 assay using a cell counting kit (CK04, Dojindo Laboratories, Kumamoto, Japan) (Zhou et al., 2021). Following 72h of culture, cells were supplemented with 10 μL CCK-8 reagents before 2h culture at 37°C. The absorbance values at 450 nm were detected on a microplate reader (Bio-Rad, Hercules, CA, USA) to evaluate cell viability. Cell viability (%)=absorbance (treated well)/absorbance (control well) ×100%.

Flow cytometry

Cells (2×10^6) were centrifuged at 1500 rpm for 3 min with 1 mL phosphate buffer saline (PBS), followed by 2 washes. After being resuspended with 300 μL pre-chilled 1×Binding Buffer, the cells in each tube were supplemented with 3 μL Annexin V-fluorescein isothiocyanate and 5 μL propidium iodide (AP101-100-kit, MULTI SCIENCES, Hangzhou, China), mixed, and cultured for 10 min in the dark at room temperature. Thereafter, cells were mixed completely with pre-chilled 1×Binding Buffer (200 μL/tube) and tested on a flowmeter (NovoCyte 2060R, ACEA Biosciences Inc., Hangzhou, China) (Mao et al., 2022).

Enzyme-linked immunosorbent assay (ELISA)

IL-8, tumor necrosis factor-α (TNF-α), and IL-6 levels were assessed in cell supernatants using the corresponding ELISA kits (PI640, PT518, and PI330, Beyotime) following the manufacturer's protocols (Sui et al., 2019).

Animals

Twenty-four SD male rats (Vital River Laboratories, Beijing, China; aged 6 weeks) were placed in individual cages with a 12/12h light/dark cycle, free access to water and food, and humidity of 50-55% at the temperature of 20-23°C. All studies obeyed the principles of the Guide for the Care and Use of Laboratory Animals and were ratified by the ethics committee of Loudi Hospital Affiliated to the University of South China & Loudi Central Hospital.

OA rat model

An anterior cruciate ligament transection and partial medial meniscectomy were adopted to establish a rat model of OA. To begin with, rats were injected intraperitoneally with pentobarbital (35 mg/kg) for anesthesia, and the medial ligament was exposed by a 1-cm longitudinal incision in the medial of the right knee joint. Then, after removal of the anterior cruciate ligament (ACL) and medial meniscus, the joint capsule and skin were sutured in a sterile environment. Rats were assigned as follows: the sham group (rats with the same incision but without excision of ACL or meniscus), the OA group, the ago-miR-105-5p group (OA rats with intra-articular injection of miR-105-5p agonist in the knee), and the ago-NC group (OA rats with intra-articular injection of agonist NC). At 4 weeks after surgery, rats were anesthetized intraperitoneally with pentobarbital and euthanized by cervical dislocation with knee cartilage tissues harvested for subsequent experimentations (Fan et al., 2021).

Hematoxylin-eosin (HE) staining

The pathological changes of the rat knee joint were evaluated and observed using HE staining (Zhou et al., 2019; Xiao et al., 2021). Sections were dehydrated with gradient alcohol, cleared with xylene, and rinsed with deionized water. Next, sections were stained with hematoxylin for 3-5 min and rinsed with deionized

water. Sections were differentiated with 1% hydrochloric acid alcohol for 20 s, returned to blue with 1% ammonia for 30 s, and rinsed with deionized water. Sections were counterstained with 1% eosin solution for 5 min and rinsed with tap water for 5 min and with deionized water for 1 min. Afterward, sections underwent dehydration with 75%, 90%, 95%, and anhydrous ethanol (5 min each) and xylene clearing (2×10 min). Finally, the sections were dried, sealed, and observed and photographed under the microscope.

TdT-mediated dUTP-biotin nick end-labeling (TUNEL)

A TUNEL kit (APT110, Roche Diagnostics GmbH, Mannheim, Germany) was applied to assess apoptosis in cartilage tissues (Zheng et al., 2005). Paraffin cartilage tissue sections (4 μm) were dewaxed with xylene, hydrated with ethanol, and rinsed 2×5 min with PBS. Then, sections were supplemented with protein K working solution for 20-min reaction at room temperature, rinsed for 2×3 min with PBS, and sealed for 10 min. Finally, sections were supplemented with 50 μL TUNEL reaction solution (a mixture of 50 μL TdT and 450 μL fluorescein-labeled dUTP) and placed in a dark wet box at 37°C for 1h before observation using fluorescence microscopy and counting of apoptotic cells.

Statistical analysis

Statistical analysis was carried out using GraphPad

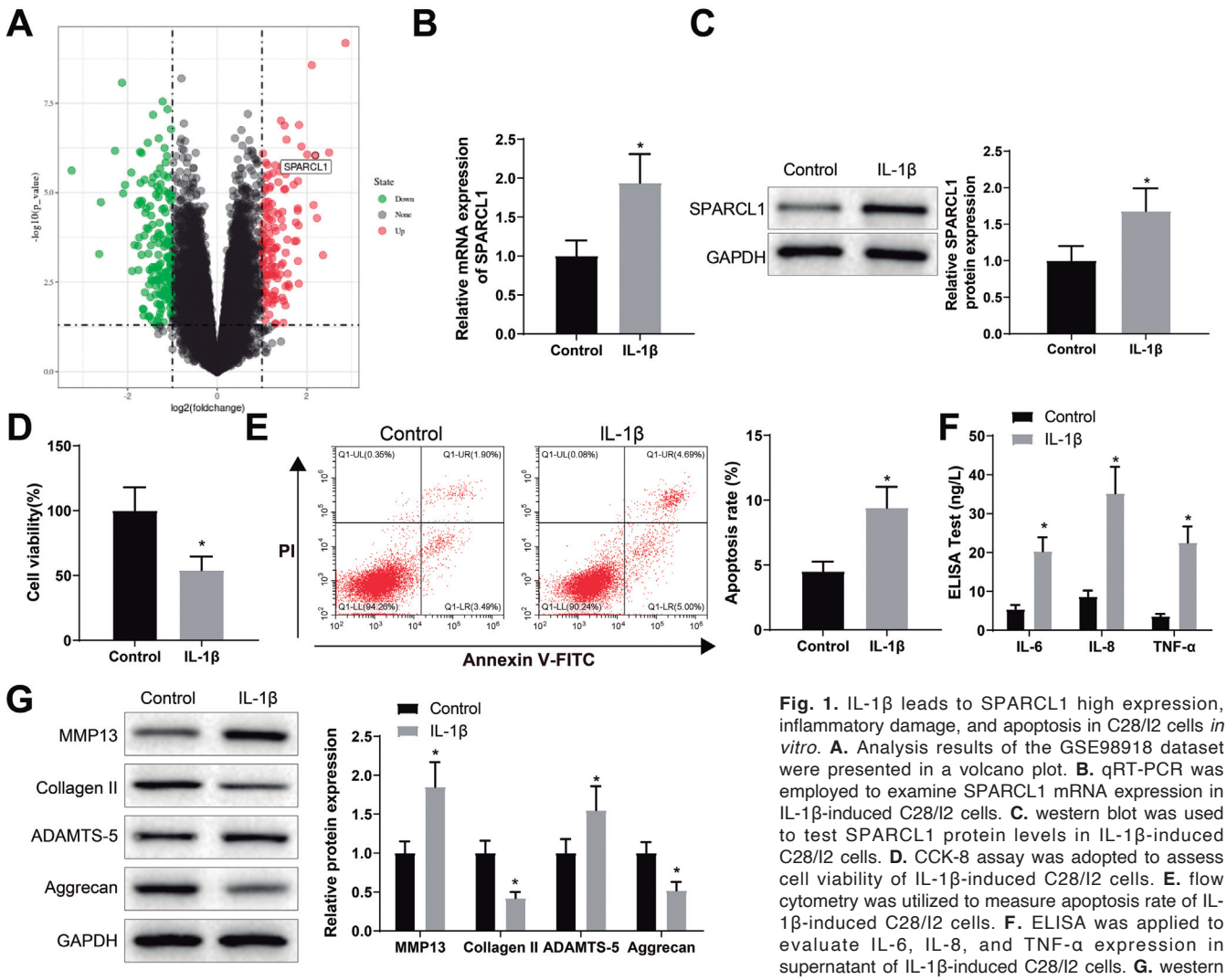

Fig. 1. IL-1β leads to SPARCL1 high expression, inflammatory damage, and apoptosis in C28/I2 cells *in vitro*. **A.** Analysis results of the GSE98918 dataset were presented in a volcano plot. **B.** qRT-PCR was employed to examine SPARCL1 mRNA expression in IL-1β-induced C28/I2 cells. **C.** western blot was used to test SPARCL1 protein levels in IL-1β-induced C28/I2 cells. **D.** CCK-8 assay was adopted to assess cell viability of IL-1β-induced C28/I2 cells. **E.** flow cytometry was utilized to measure apoptosis rate of IL-1β-induced C28/I2 cells. **F.** ELISA was applied to evaluate IL-6, IL-8, and TNF-α expression in supernatant of IL-1β-induced C28/I2 cells. **G.** western blot was used to test MMP13, ADAMTS-5, Collagen II, and Aggrecan protein levels in IL-1β-induced C28/I2 cells. **P*<0.05 compared to the control group. The above results were measurement data which were expressed as mean ± standard deviation. The independent sample t-test was used for comparison between the two groups. N=3. SPARCL1, secreted protein, acidic and rich in cysteine-like 1; IL, interleukin; TNF, tumor necrosis factor; MMP13, matrix metalloproteinase 13; ADAMTS, A Disintegrin and Metalloproteinase with ThromboSpondin motifs.

prism8 software with data displayed as mean ± standard deviation. The t-test was employed for comparisons between two groups, and one-way analysis of variance test for comparisons among multiple groups, with Tukey's test for post hoc multiple comparisons. $P<0.05$ was viewed to be statistically significant for the difference.

Results

SPARCL1 expression was high in the IL-1β-induced OA model in vitro

To identify differential genes in OA, the GSE98918 microarray was analyzed, which manifested that SPARCL1 expression was appreciably upregulated in OA tissues versus non-OA tissues (Fig. 1A). C28/I2 cells received IL-1β (10 ng/mL) stimulation to construct an *in vitro* OA model. As presented, SPARCL1 expression in C28/I2 cells was noticeably upregulated after IL-1β stimulation (Fig. 1B,C). As exhibited in Figure 1D, CCK-8 assay displayed a decline in cell viability after IL-1β stimulation. The flow cytometry results exhibited that cell apoptosis was remarkably elevated after IL-1β stimulation (Fig. 1E). ELISA data presented that IL-6, IL-8, and TNF-α levels were dramatically augmented in the cell supernatant after IL-1β stimulation (Fig. 1F). Western blot was utilized to evaluate protein expression of cartilage matrix degradation markers (MMP13, Collagen II, ADAMTS-5, and Aggrecan). The results in

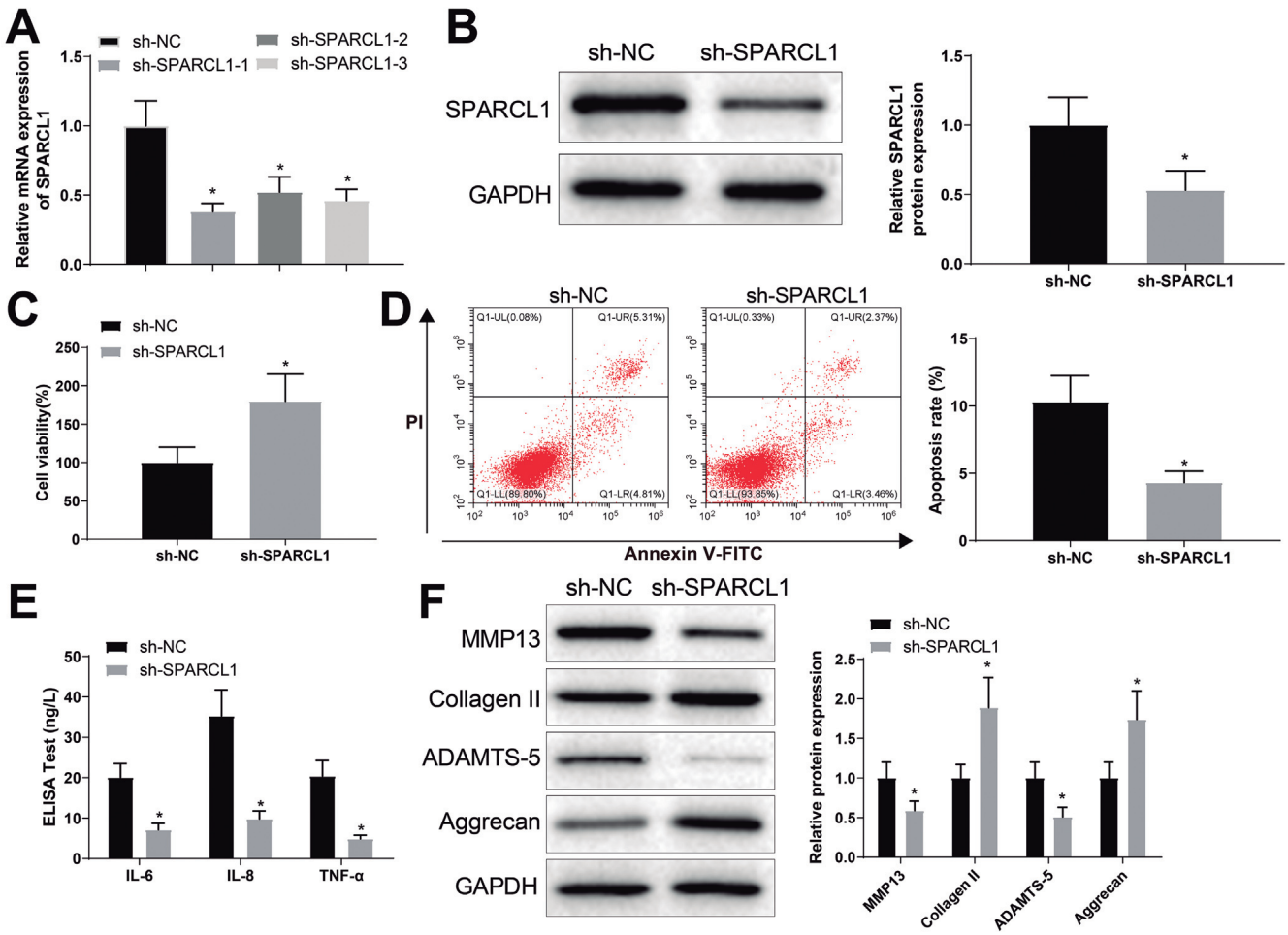

Fig. 2. IL-1β-induced chondrocyte injury and extracellular matrix degradation are repressed by SPARCL1 knockdown. After C28/I2 cells were transfected with sh-SPARCL1 and then induced with IL-1β. **A.** qRT-PCR was conducted to examine the knockdown efficiency of sh-SPARCL1. **B.** western blot was carried out to test SPARCL1 protein levels. **C.** CCK-8 assay was performed to assess cell viability. **D.** flow cytometry was used to measure apoptosis rate. **E.** ELISA was implemented to evaluate IL-6, IL-8, and TNF-α expression in cell supernatant. **F.** western blot was carried out to test MMP13, ADAMTS-5, Collagen II, and Aggrecan protein levels. *$P<0.05$ compared to the sh-NC group. The above results were measurement data which were expressed as mean ± standard deviation. The independent sample t-test was used for comparison between the two groups, and one-way analysis of variance test for comparison among multiple groups, with Tukey's test for post hoc multiple comparisons. N=3. SPARCL1, secreted protein, acidic and rich in cysteine-like 1; IL, interleukin; TNF, tumor necrosis factor; MMP13, matrix metalloproteinase 13; ADAMTS, A Disintegrin and Metalloproteinase with ThromboSpondin motifs.

Figure 1G indicated that MMP13 and ADAMTS-5 protein expression was remarkably enhanced and Collagen II and Aggrecan protein levels were considerably downregulated in C28/I2 cells after IL-1β stimulation. Therefore, SPARCL1 expression was high and chondrocyte injury and ECM degradation were induced in C28/I2 cells with IL-1β stimulation.

SPARCL1 knockdown restricted IL-1β-induced chondrocyte injury and ECM degradation

To delve into the function of SPARCL1 in C28/I2 cells with IL-1β stimulation, three shRNA sequences were designed to knock down SPARCL1 expression in the cells. The qRT-PCR results described that sh-SPARCL1-1 exhibited a relatively better knockdown effect (Fig. 2A) and, therefore, was chosen for the following experiments (subsequently referred to as sh-SPARCL1). Western blot results displayed that sh-SPARCL1 conspicuously reduced SPARCL1 protein expression in C28/I2 cells with IL-1β stimulation (Fig. 2B). CCK-8 and flow cytometry assays presented that SPARCL1 knockdown dramatically enhanced viability but diminished apoptosis in C28/I2 cells with IL-1β stimulation (Fig. 2C,D). ELISA manifested that SPARCL1 knockdown appreciably reduced IL-1β-triggered production of IL-6, TNF-α, and IL-8 in C28/I2 cells (Fig. 2E). Western blot depicted that SPARCL1

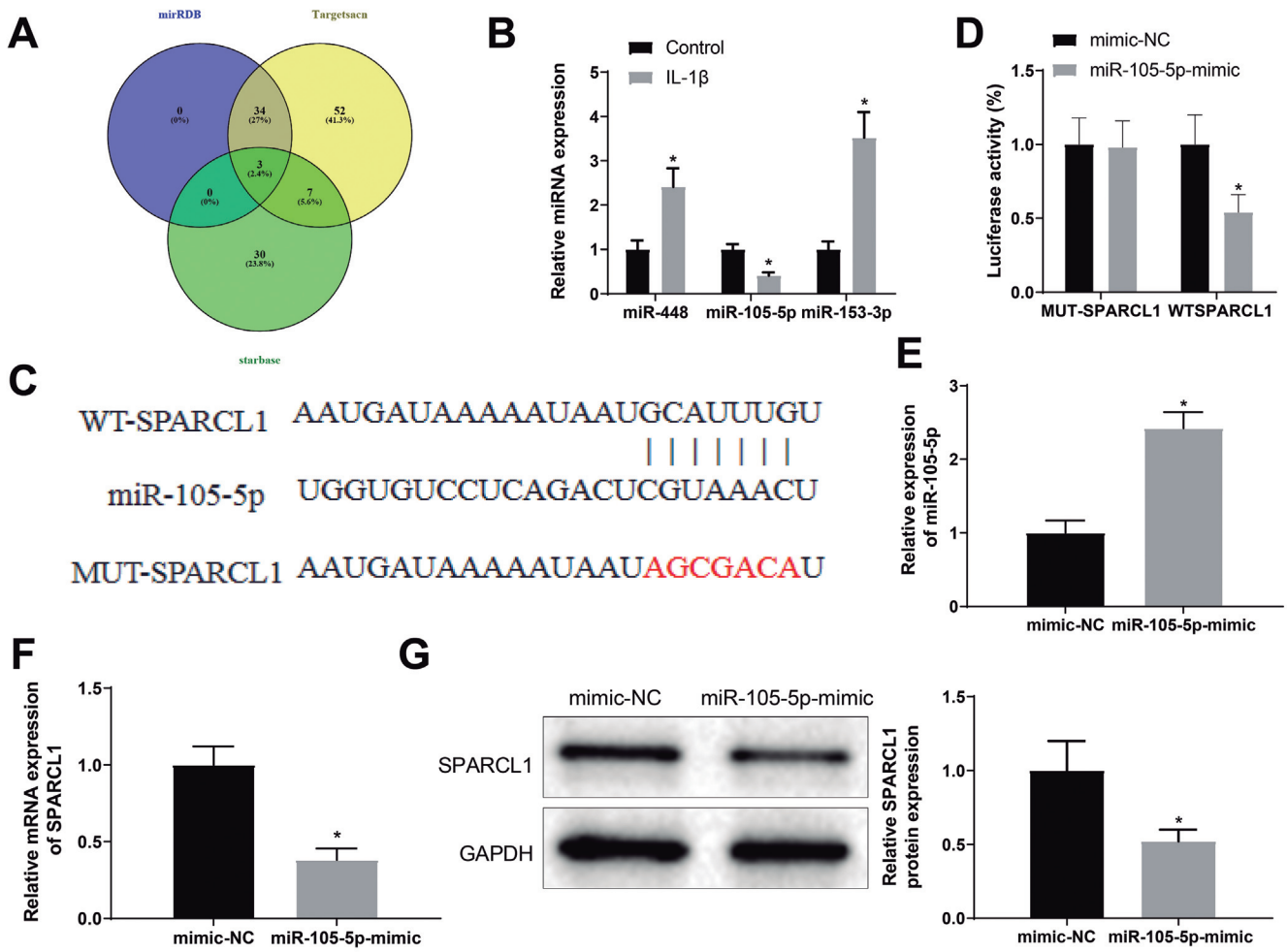

Fig. 3. SPARCL1 is negatively targeted by miR-105-5p. **A.** Intersection of predicted upstream miRNAs targeting SPARCL1 was demonstrated using a Venn diagram. **B.** qRT-PCR was employed to detect the expression of the predicted miRNAs in IL-1β-stimulated C28/I2 cells. **C.** the binding sites of miR-105-5p to SPARCL1 was predicted by Starbase. **D.** the binding relationship was analyzed using the dual-luciferase reporter assay. **E.** qRT-PCR was employed to detect miR-105-5 expression in IL-1β-stimulated C28/I2 cells after miR-105-5p-mimic treatment. **F.** qRT-PCR was employed to detect SPARCL1 mRNA expression in IL-1β-stimulated C28/I2 cells after miR-105-5p-mimic treatment. **G.** western blot was adopted to determine SPARCL1 protein expression in IL-1β-stimulated C28/I2 cells after miR-105-5p-mimic treatment. **P*<0.05 compared to the control or mimic-NC group. The above results were measurement data which were expressed as mean ± standard deviation. The independent sample t-test was used for comparison between the two groups. N=3. SPARCL1, secreted protein, acidic and rich in cysteine-like 1; IL, interleukin; NC, negative control.

knockdown diminished MMP13 and ADAMTS-5 expression and augmented Collagen II and Aggrecan protein levels in C28/I2 cells with IL-1β stimulation (Fig. 2F). In conclusion, SPARCL1 knockdown curtailed chondrocyte injury and ECM degradation in C28/I2 cells with IL-1β stimulation.

miR-105-5p inversely targeted SPARCL1

In order to further probe into the prospective mechanism of SPARCL1 in OA, upstream miRNAs targeting SPARCL1 were predicted using miRDB, Targetscan, and Starbase database, and the intersection of miRNAs was attained by plotting Venn diagrams through the Venny2.1 online website (miR-448, miR-105-5p, and miR-153-3p) (Fig. 3A). The expression of the three miRNAs in C28/I2 cells with IL-1β stimulation was examined by qRT-PCR, which exhibited high miR-448 and miR-153-3p expression and low miR-105-5p expression (Fig. 3B). Therefore, miR-105-5p of interest was utilized for subsequent experiments.

The WT-SPARCL1 and MUT-SPARCL1 with miR-105-5p binding sites were designed and synthesized according to the prediction results of the Starbase database (Fig. 3C). Subsequently, the targeting relationship was verified using the dual-luciferase reporter assay. As exhibited in Figure 3D, miR-105-5p-mimic transfection dramatically diminished luciferase activity in WT-SPARCL1, whilst that of MUT-SPARCL1 did not change subsequent to miR-105-5p-mimic transfection.

miR-105-5p-mimic or mimic-NC was transfected into C28/I2 cells, followed by stimulation with IL-1β. qRT-PCR manifested that miR-105-5p-mimic transfection signally upregulated miR-105-5p expression in C28/I2 cells with IL-1β stimulation (Fig. 3E), indicating a favorable transfection efficiency. Moreover, SPARCL1 mRNA and protein levels were substantially lowered by miR-105-5p-mimic in C28/I2 cells with IL-1β stimulation (Fig. 3F,G). Collectively, miR-105-5p targeted SPARCL1 to downregulate SPARCL1.

miR-105-5p overexpression impeded IL-1β-induced chondrocyte injury and ECM degradation

Subsequently, the study probed the role of miR-105-5p in C28/I2 cells with IL-1β stimulation. CCK-8 assay and flow cytometry highlighted that miR-105-5p-mimic transfection markedly enhanced cell viability and lowered apoptosis of C28/I2 cells with IL-1β stimulation (Fig. 4A,B). ELISA results proposed that miR-105-5p-mimic transfection contributed to remarkable reductions

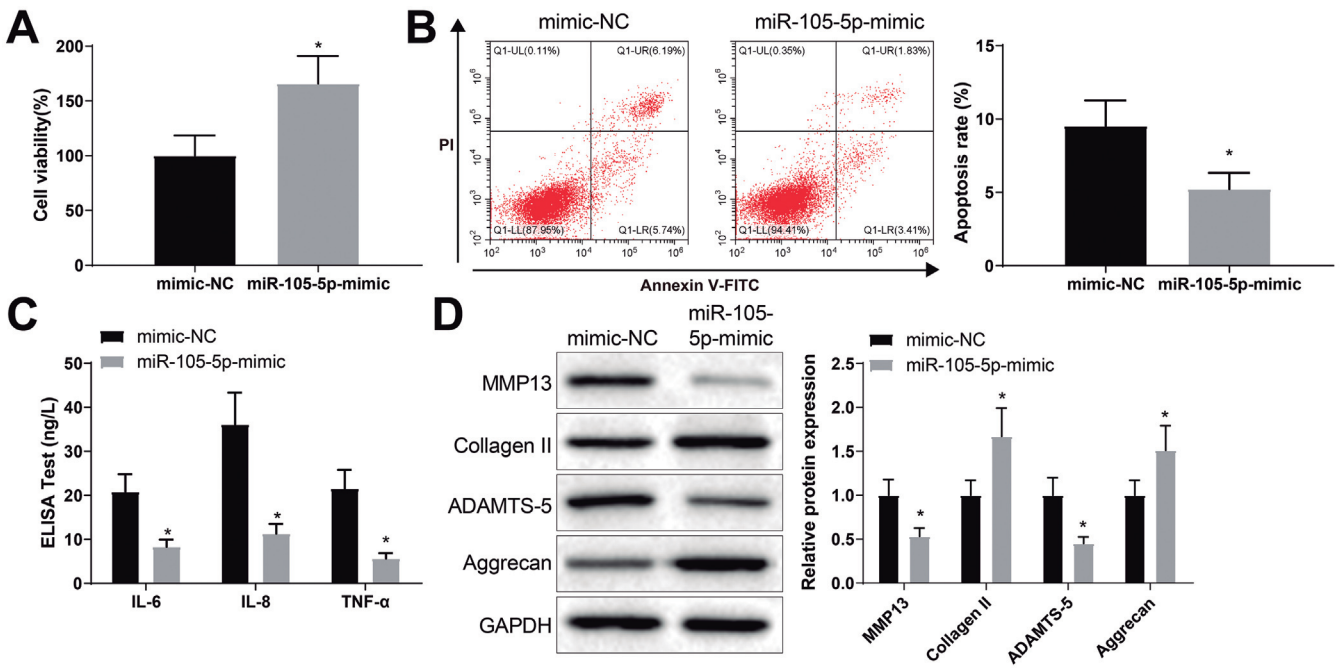

Fig. 4. IL-1β-induced chondrocyte injury and extracellular matrix degradation in C28/I2 cells are retarded by upregulating miR-105-5p. After treatment of miR-105-5p-mimic and induction of IL-1β in C28/I2 cells. **A.** CCK-8 assay was employed to detect cell viability. **B.** flow cytometry was implemented to test apoptosis rate. **C.** ELISA was utilized to examine IL-6, IL-8, and TNF-α level in cell supernatant. **D.** western blot was carried out to detect MMP13, ADAMTS-5, Collagen II, and Aggrecan protein levels. **P*<0.05 compared to the mimic-NC group. The above results were measurement data which were expressed as mean ± standard deviation. The independent sample t-test was applied for comparison between the two groups. N=3. IL, interleukin; NC, negative control; TNF, tumor necrosis factor; MMP13, matrix metalloproteinase 13; ADAMTS, A Disintegrin and Metalloproteinase with ThromboSpondin motifs.

of IL-1β-triggered production of IL-6, TNF-α, and IL-8 in C28/I2 cells (Fig. 4C). As discovered in western blot results, overexpression of miR-105-5p lessened ADAMTS-5 and MMP13 expression and augmented Aggrecan and Collagen II protein levels in C28/I2 cells with IL-1β stimulation (Fig. 4D). In summary, miR-105-5p overexpression restricted chondrocyte injury and ECM degradation induced by IL-1β in C28/I2 cells.

miR-105-5 overexpression subdued IL-1β-induced chondrocyte injury and ECM degradation by targeting SPARCL1

To further ascertain whether miR-105-5p functioned in C28/I2 cells with IL-1β stimulation via SPARCL1, C28/I2 cells were co-transfected with miR-105-5p-mimic and oe-SPARCL1/oe-NC before IL-1β stimulation. In C28/I2 cells with IL-1β stimulation, oe-SPARCL1 transfection prominently upregulated SPARCL1 mRNA and protein levels in the presence of miR-105-5p-mimic transfection (Fig. 5A,B). Besides, CCK-8 results elaborated that oe-SPARCL1 transfection abrogated the promotion of IL-1β-stimulated C28/I2 cell viability caused by miR-105-5p-mimic (Fig. 5C). Flow cytometry revealed that oe-SPARCL1 transfection reversed the suppression of IL-1β-stimulated C28/I2 cell apoptosis triggered by miR-105-5p-mimic (Fig. 5D). ELISA results displayed that oe-SPARCL1 transfection counteracted the repressive impacts of miR-105-5p-mimic on inflammatory factor secretion in IL-1β-stimulated C28/I2 cell supernatants (Fig. 5E). With regard to western blot data, oe-SPARCL1 transfection enhanced the protein levels of cartilage matrix degradation markers in C28/I2 cells with IL-1β

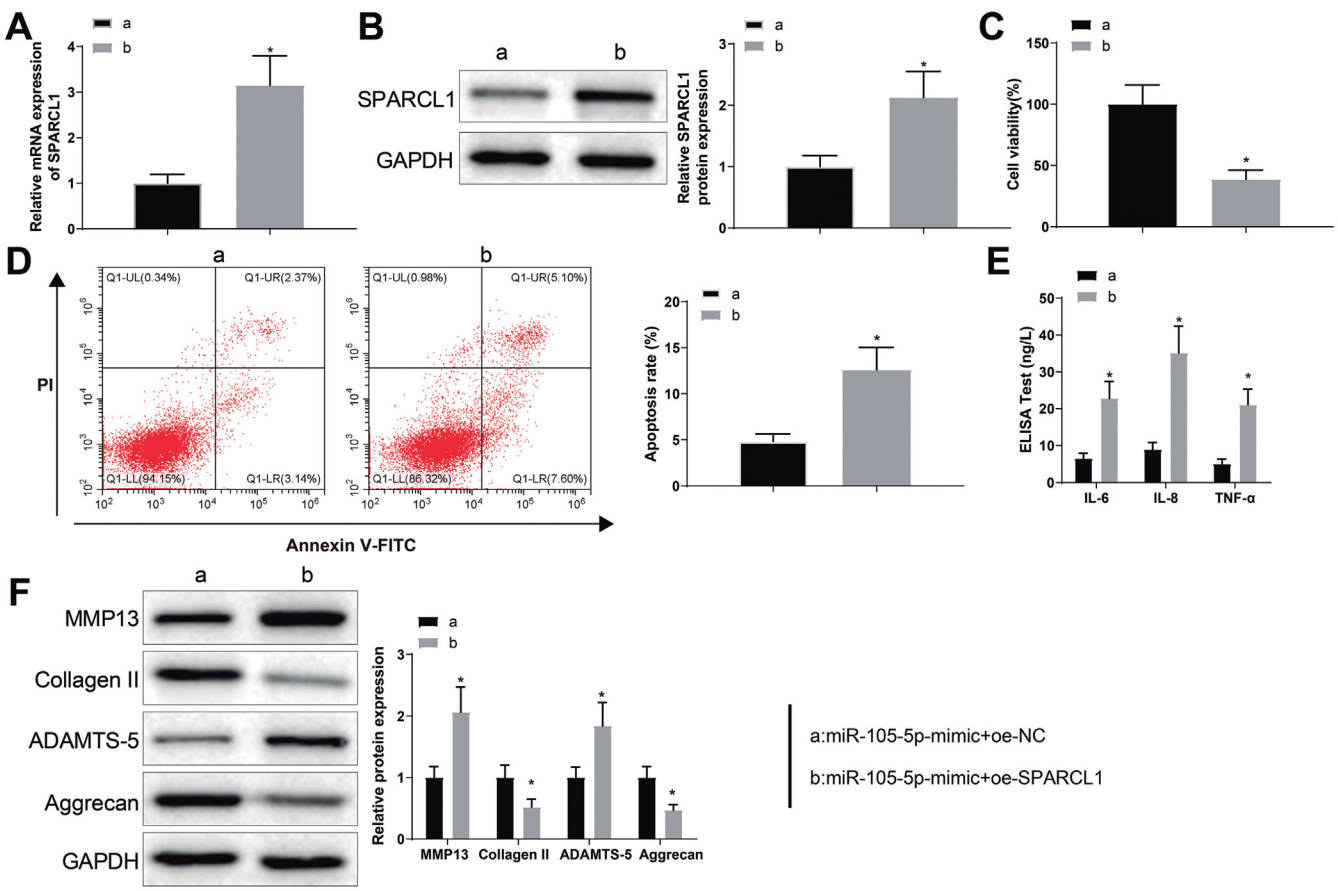

Fig. 5. miR-105-5p/SPARCL1 axis modulates IL-1β-induced chondrocyte injury and extracellular matrix degradation. After C28/I2 cells were co-transfected with miR-105-5p-mimic and oe-SPARCL1/oe-NC and stimulated with IL-1β. **A.** qRT-PCR was utilized to measure SPARCL1 mRNA expression. **B.** western blot was performed to detect SPARCL1 protein level. **C.** CCK-8 assay was implemented to determine cell viability. **D.** flow cytometry was employed to test apoptosis rate. **E.** ELISA was applied to assess IL-6, IL-8, and TNF-α expression in cell supernatant. **F.** western blot was carried out to evaluate MMP13, ADAMTS-5, Collagen II, and Aggrecan protein levels. **P*<0.05 compared to the miR-105-5p-mimic + oe-NC group. The above results were measurement data which were expressed as mean ± standard deviation. The independent sample t-test was used for comparison between the two groups. N=3. SPARCL1, secreted protein, acidic and rich in cysteine-like 1; IL, interleukin; oe, overexpression; NC, negative control; TNF, tumor necrosis factor; MMP13, matrix metalloproteinase 13; ADAMTS, A Disintegrin and Metalloproteinase with ThromboSpondin motifs.

stimulation in the presence of miR-105-5p-mimic (Fig. 5F). In conclusion, miR-105-5p depressed IL-1β-induced chondrocyte injury and ECM degradation in C28/I2 cells by binding to SPARCL1.

Upregulation of miR-105-5p attenuated cartilage injury in OA rats

For determining whether miR-105-5p restrains the

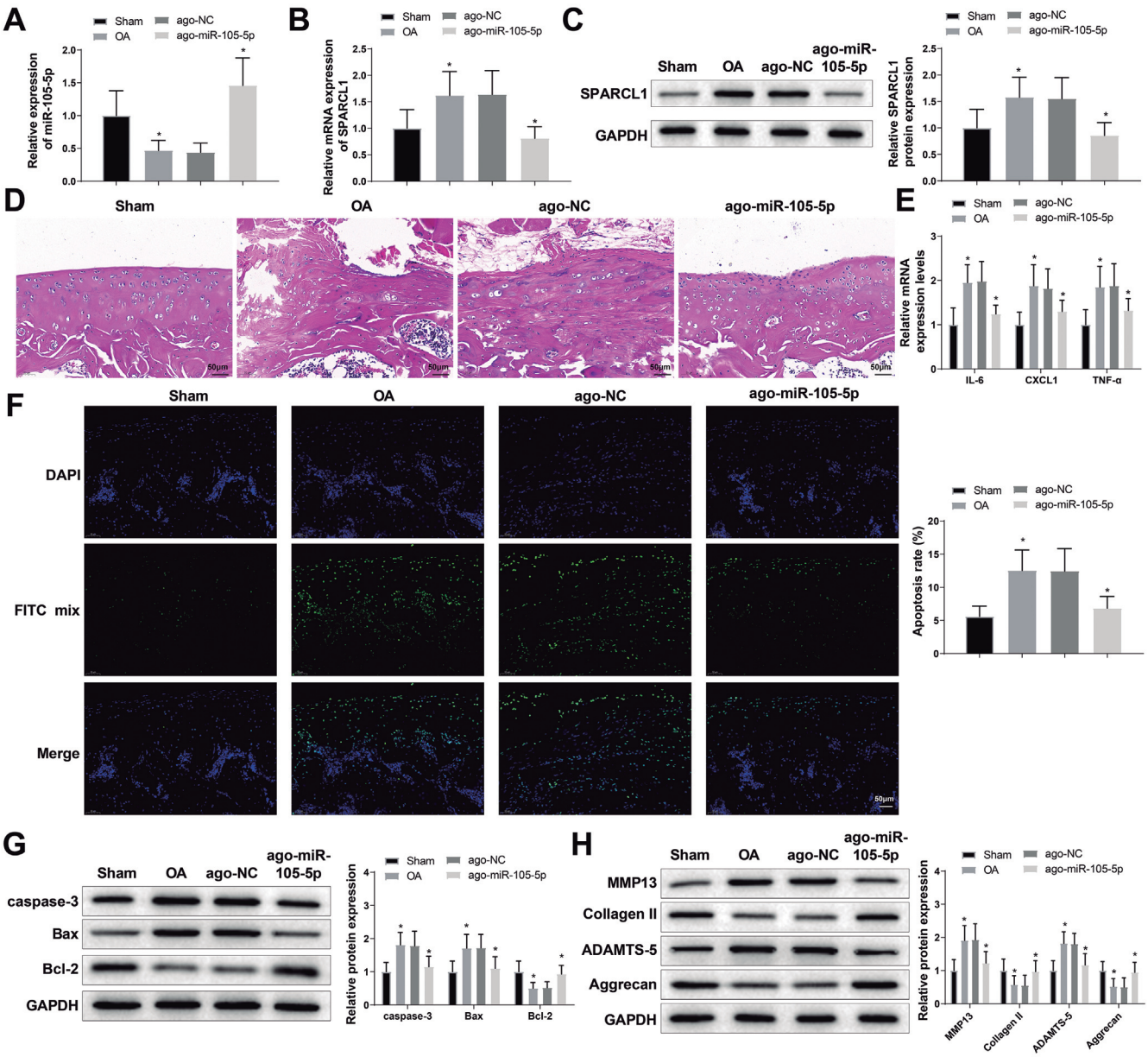

Fig. 6. Cartilage injury in OA rats is alleviated by upregulating miR-105-5p. **A.** qRT-PCR was employed to test miR-105-5p expression in rats after overexpressing miR-105-5p. **B.** qRT-PCR was adopted to measure SPARCL1 mRNA expression in rats after overexpressing miR-105-5p. **C.** western blot was utilized to detect SPARCL1 protein level in rats after overexpressing miR-105-5p. **D.** HE staining was employed to assess cartilage tissue injury in rats after overexpressing miR-105-5p. **E.** qRT-PCR was conducted to assess IL-6, CXCL1, and TNF-α expression in rats after overexpressing miR-105-5p. **F.** TUNEL was implemented to detect apoptosis in cartilage tissues of rats after overexpressing miR-105-5p. **G.** western blot was employed to evaluate Bax, Bcl-2, and caspase-3 protein levels in rats after overexpressing miR-105-5p; H: western blot was adopted to examined MMP13, Collagen II, ADAMTS-5, and Aggrecan protein levels in rats after overexpressing miR-105-5p. **P*<0.05 compared to the sham or ago-NC group. The above results were measurement data which were expressed as mean ± standard deviation. One-way analysis of variance test was applied for comparisons among multiple groups, with Tukey's multiple comparisons test for post hoc multiple comparisons. N=6 rats for each group. OA, osteoarthritis; SPARCL1, secreted protein, acidic and rich in cysteine-like 1; IL, interleukin; TNF, tumor necrosis factor; MMP13, matrix metalloproteinase 13; ADAMTS, A Disintegrin and Metalloproteinase with ThromboSpondin motifs; NC, negative control.

progression of OA *in vivo*, we established a rat model of OA. Relative to the sham group, the OA group presented a prominently lower miR-105-5p expression and higher SPARCL1 expression. Meanwhile, compared to the ago-NC group, the ago-miR-105-5p group exhibited a conspicuous elevation of miR-105-5p expression and a decrease of SPARCL1 expression, and no evident changes were found in the ago-NC and OA groups (Fig. 6A-C).

HE staining results in Figure 6D exhibited smooth cartilage surface and no cartilage sclerosis in rats of the sham group, severe cartilage tissue injury in rats of the OA and ago-NC groups, and ameliorated cartilage injury in rats of the ago-miR-105-5p group. As presented by qRT-PCR results, the mRNA levels of IL-6, CXCL1, and TNF-α were evidently higher in the OA and ago-NC groups than in the sham group, while IL-6, CXCL1, and TNF-α levels were reduced in the ago-miR-105-5p group versus the ago-NC group (Fig. 6E). TUNEL staining demonstrated fewer apoptotic cells in cartilage tissues of the sham group, as well as remarkably higher numbers of apoptotic cells in cartilage tissues of the OA and ago-NC groups than in the sham group. The ago-miR-105-5p group had considerably reduced apoptosis in contrast to the ago-NC group (Fig. 6F).

Western blot results uncovered that Bcl-2, Collagen II, and Aggrecan expression was observably diminished, whilst caspase-3, Bax, MMP13, and ADAMTS-5 expression was apparently elevated in the OA group compared to the sham group. In comparison with the ago-NC group, increased expression of Bcl-2, Collagen II, and Aggrecan and decreased expression of caspase-3, Bax, MMP13, and ADAMTS-5 were observed in the ago-miR-105-5p group (Fig. 6G,H). Collectively, miR-105-5p overexpression alleviated cartilage injury in OA rats.

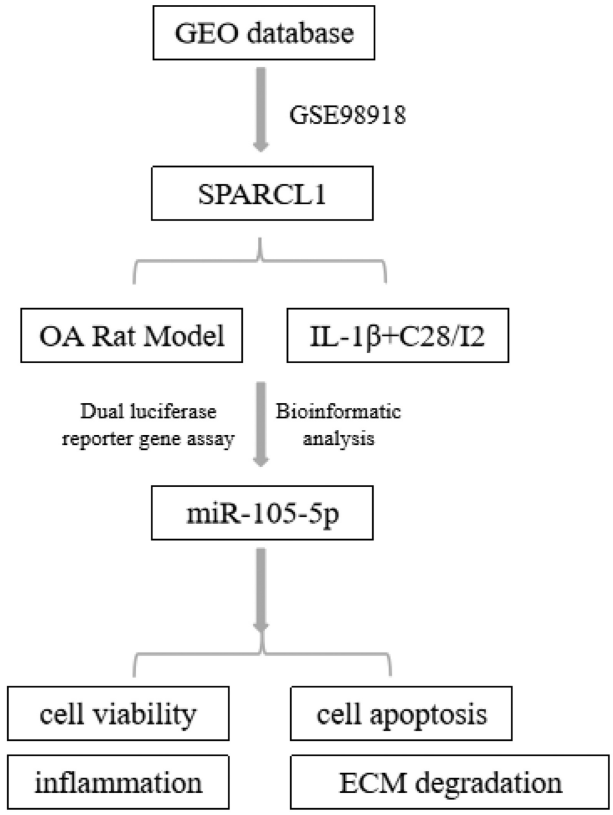

Fig. 7. Mechanism of action of miR-105-5p targeting SPARCL1 in the regulation of chondrocyte injury. Analysis of the microarray GSE98918 obtained through the GEO database revealed that SPARCL1 was highly expressed in OA patients, and bioinformatics analysis and dual-luciferase reporter gene assays identified that miR-105-5p targeted SPARCL1. An *in vitro* model of OA was constructed through IL-1β stimulation of C28/I2 cells. IL-1β inhibited C28/I2 cell viability and promoted cell apoptosis, inflammation, and cartilage matrix degradation. miR-105-5p overexpression or SPARCL1 silencing significantly reversed the decrease in viability and elevation in apoptosis in IL-1β-treated C28/I2 cells and diminished inflammatory factor expression and cartilage matrix degradation. Furthermore, the upregulation of SPARCL1 abolished the effects of miR-105-5p mimics on IL-1β-induced C28/I2 cell viability, apoptosis, and inflammation. An *in vivo* model of OA was established with the anterior cruciate ligament transection and partial medial meniscectomy. *In vivo* upregulation of miR-105-5p attenuated knee cartilage tissue injury in OA rats.

Discussion

OA, as a disease related to pain and disability in adults, is accompanied by abnormal changes in the meniscus, articular cartilage, synovial tissue, and subchondral bone (Ghafouri-Fard et al., 2021). Moreover, OA is one of the few most prevalent chronic aging and articular disorders for which there are few effective therapies, and no approach has been validated to delay the progression of osteoarthritis (Jang et al., 2021). Therefore, research on the mechanisms behind OA progression is necessary for the development of effective treatments. This study uncovered that miR-105-5p constrained chondrocyte apoptosis, inflammation, and injury, ECM degradation, and OA progression by downregulating SPARCL1.

An article illustrates that ECM mainly consists of Aggrecan proteoglycans and Collagen II which respectively provide flexibility and strength to the tissues (Thomson and Hilkens, 2021). Increased expression of ECM catabolic enzymes (ADAMTS-5 and MMP-13), inflammatory cytokines (IL-1β, TNF, and IL-6), and apoptotic genes (caspase-3) and decreased expression of anabolic genes (Aggrecan and Collagen II) all result in cartilage degeneration, synovium inflammation, and consequently articular aches, stiffness, and impaired mobility in OA (Endisha et al., 2021). Therefore, the degree of OA in this study was determined by detecting the expression of these indicators in OA cells or tissues. In addition, IL-1β is able to affect cartilage-degrading enzyme (MMPs) production, ECM synthesis, and the expression of other pro-inflammatory cytokines in OA tissues (Chien et al.,

2020). Accumulating evidence has unraveled that IL-1β is widely utilized to construct an *in vitro* model of OA (Fei et al., 2019; Wang et al., 2019; He et al., 2020). Therefore, IL-1β induction was employed to successfully construct an OA model *in vitro* to investigate the underpinning mechanisms in OA. Similarly, Collagen II and Aggrecan protein levels were lowered, and ADAMTS-5 and MMP-13 expressions, inflammatory factor levels, and apoptosis were increased in the IL-1β-induced OA cell model, as detected in our research.

SPARCL1 expression has been measured in OA by several studies. For instance, Sieker et al. found that SPARC is abundantly expressed in articular cartilage after surgically induced early post-traumatic OA (Sieker et al., 2018). A prior publication deciphered that OA meniscus had elevated SPARCL1 expression (Brophy et al., 2018). Likewise, the research of Balakrishnant et al. unveiled that the synovial fluid of OA also exhibited high expression of SPARCL1 (Balakrishnan et al., 2014). Consistently, this study also identified that SPARCL1 expression was elevated in the *in vitro* OA model induced by IL-1β. Nevertheless, no studies have yet been conducted to dissect the specific function of SPARCL1 in OA development. A prior study revealed that SPARCL1 prevalently existed in astrocytes expressing IL-1β and ADAMTS4 (Lively et al., 2011). Partially, our experimental data uncovered that knockdown of SPARCL1 decreased IL-8 and ADAMTS-5 expression in C28/I2 cells with IL-1β stimulation. Additionally, our research first demonstrated that SPARCL1 knockdown restricted apoptosis, diminished IL-6, TNF-α, ADAMTS-5, and MMP13 expression, and elevated Aggrecan and Collagen II expression and viability in C28/I2 cells with IL-1β stimulation, indicating that silencing of SPARCL1 repressed IL-1β-induced chondrocyte injury and ECM degradation.

For the deep exploration of the mechanism of SPARCL1 in OA development, a targeting relationship between miR-105-5p and SPARCL1 was predicted by the Starbase website and verified by dual-luciferase reporter assay. Numerous miRNAs have been discovered to modulate cell viability, differentiation, matrix-degrading enzymes, and inflammatory cytokine production in cartilage (Ito et al., 2021). A previous paper discovered that patients with knee OA had low hsa-miR-105-5p expression in plasma (Weng et al., 2020). Concordantly, our data presented that miR-105-5p was lowly expressed in C28/I2 cells with IL-1β stimulation. Moreover, miR-105 overexpression restrained the production of ADAMTSs such as ADAMTS5 and augmented Aggrecan expression in chondrocytes and articular cartilage degeneration (Ji et al., 2016). Likewise, our research proposed that miR-105-5p overexpression repressed cartilage matrix degradation, apoptosis, and inflammation and accelerated viability of C28/I2 cells with IL-1β stimulation. In addition, the mitigating impacts of miR-105 overexpression on inflammation, apoptosis, and cartilage injury were also confirmed in a rat model of OA. Subsequently, rescue assays highlighted that the effect of overexpressing miR-105-5p on IL-1β-induced C28/I2 cells was nullified by upregulation of SPARCL1.

In summary, our study first identified an association between SPARCL1 and OA progression. Moreover, our data revealed that miR-105-5p suppressed IL-1β-induced apoptosis, inflammation, and injury of chondrocytes and ECM degradation by reducing SPARCL1 expression. Also, miR-105-5p inhibited cartilage injury in OA rats (Fig. 7). Our findings indicate a promising target for the development of novel management and drugs for OA to improve the suffering and quality of life of the OA population. Naturally, the upstream and downstream targets of miR-105-5p/SPARCL1 axis were not explored in more detail in this paper, which merits further research in the future.

Acknowledgements. Not applicable.

Declaration of interest. The authors declare that they have no competing interests.

Funding. This research was funded by the Natural Science Foundation of Hunan Province (Grant No. 2022JJ30574 and No. 2023JJ50507).

References

Balakrishnan L., Nirujogi R.S., Ahmad S., Bhattacharjee M., Manda S.S., Renuse S., Kelkar D.S., Subbannayya Y., Raju R., Goel R., Thomas J.K., Kaur N., Dhillon M., Tankala S.G., Jois R., Vasdev V., Ramachandra Y., Sahasrabuddhe N.A., Prasad Ts K., Mohan S., Gowda H., Shankar S. and Pandey A. (2014). Proteomic analysis of human osteoarthritis synovial fluid. Clin. Proteomics 11, 6.

Brophy R.H., Zhang B., Cai L., Wright R.W., Sandell L.J. and Rai M.F. (2018). Transcriptome comparison of meniscus from patients with and without osteoarthritis. Osteoarthritis Cartilage 26, 422-432.

Chen D., Shen J., Zhao W., Wang T., Han L., Hamilton J.L. and Im H.J. (2017). Osteoarthritis: Toward a comprehensive understanding of pathological mechanism. Bone Res. 5, 16044.

Chen S., Zou Q., Chen Y., Kuang X., Wu W., Guo M., Cai Y. and Li Q. (2020). Regulation of SPARC family proteins in disorders of the central nervous system. Brain Res. Bull. 163, 178-189.

Chien S.Y., Tsai C.H., Liu S.C., Huang C.C., Lin T.H., Yang Y.Z. and Tang C.H. (2020). Noggin inhibits IL-1β and BMP-2 expression, and attenuates cartilage degeneration and subchondral bone destruction in experimental osteoarthritis. Cells 9, 927.

Delplace V., Boutet M.A., Le Visage C., Maugars Y., Guicheux J. and Vinatier C. (2021). Osteoarthritis: From upcoming treatments to treatments yet to come. Joint Bone Spine 88, 105206.

Ding Y., Wang L., Zhao Q., Wu Z. and Kong L. (2019). MicroRNA-93 inhibits chondrocyte apoptosis and inflammation in osteoarthritis by targeting the TLR4/NF-κB signaling pathway. Int. J. Mol. Med. 43, 779-790.

Disease G.B.D., Injury I. and Prevalence C. (2018). Global, regional, and national incidence, prevalence, and years lived with disability for 354 diseases and injuries for 195 countries and territories, 1990-2017: A systematic analysis for the Global Burden of Disease Study 2017. Lancet 392, 1789-1858.

Endisha H., Datta P., Sharma A., Nakamura S., Rossomacha E., Younan C., Ali S.A., Tavallaee G., Lively S., Potla P., Shestopaloff K., Rockel J.S., Krawetz R., Mahomed N.N., Jurisica I., Gandhi R. and Kapoor M. (2021). MicroRNA-34a-5p promotes joint destruction during osteoarthritis. Arthritis Rheumatol. 73, 426-439.

Fan G., Liu J., Zhang Y. and Guan X. (2021). LINC00473 exacerbates osteoarthritis development by promoting chondrocyte apoptosis and proinflammatory cytokine production through the miR-424-5p/LY6E axis. Exp. Ther. Med. 22, 1247.

Fei J., Liang B., Jiang C., Ni H. and Wang L. (2019). Luteolin inhibits IL-1β-induced in flammation in rat chondrocytes and attenuates osteoarthritis progression in a rat model. Biomed. Pharmacother. 109, 1586-1592.

Feng W., Huang W., Chen J., Qiao C., Liu D., Ji X., Xie M., Zhang T., Wang Y., Sun M., Tian D., Fan D., Nie Y., Wu K. and Xia L. (2021). CXCL12-mediated HOXB5 overexpression facilitates colorectal cancer metastasis through transactivating CXCR4 and ITGB3. Theranostics 11, 2612-2633.

Gagliardi F., Narayanan A. and Mortini P. (2017). SPARCL1 a novel player in cancer biology. Crit. Rev. Oncol. Hematol. 109, 63-68.

Ghafouri-Fard S., Poulet C., Malaise M., Abak A., Mahmud Hussen B., Taheriazam A., Taheri M. and Hallajnejad M. (2021). The emerging role of non-coding RNAs in osteoarthritis. Front. Immunol. 12, 773171.

He L., He T., Xing J., Zhou Q., Fan L., Liu C., Chen Y., Wu D., Tian Z., Liu B. and Rong L. (2020). Bone marrow mesenchymal stem cell-derived exosomes protect cartilage damage and relieve knee osteoarthritis pain in a rat model of osteoarthritis. Stem Cell Res. Ther. 11, 276.

Hermann W., Lambova S. and Muller-Ladner U. (2018). Current treatment options for osteoarthritis. Curr. Rheumatol. Rev. 14, 108-116.

Huang Y., Zhou J., Hakamivala A., Wu J., Hong Y., Borrelli J. and Tang L. (2017). An optical probe for detecting chondrocyte apoptosis in response to mechanical injury. Sci. Rep. 7, 10906.

Ito Y., Matsuzaki T., Ayabe F., Mokuda S., Kurimoto R., Matsushima T., Tabata Y., Inotsume M., Tsutsumi H., Liu L., Shinohara M., Tanaka Y., Nakamichi R., Nishida K., Lotz M.K. and Asahara H. (2021). Both microRNA-455-5p and -3p repress hypoxia-inducible factor-2alpha expression and coordinately regulate cartilage homeostasis. Nat. Commun. 12, 4148.

Jang S., Lee K. and Ju J.H. (2021). Recent updates of diagnosis, pathophysiology, and treatment on osteoarthritis of the knee. Int. J. Mol. Sci. 22, 2619.

Jena A., Taneja S., Rana P., Goyal N., Vaish A., Botchu R. and Vaishya R. (2021). Emerging role of integrated PET-MRI in osteoarthritis. Skeletal Radiol. 50, 2349-2363.

Ji Q., Xu X., Xu Y., Fan Z., Kang L., Li L., Liang Y., Guo J., Hong T., Li Z., Zhang Q., Ye Q. and Wang Y. (2016). MiR-105/Runx2 axis mediates FGF2-induced ADAMTS expression in osteoarthritis cartilage. J. Mol. Med. (Berl). 94, 681-694.

Li Q., Wu M., Fang G., Li K., Cui W., Li L., Li X., Wang J. and Cang Y. (2021). MicroRNA-186-5p downregulation inhibits osteoarthritis development by targeting MAPK1. Mol. Med. Rep. 23, 253.

Lin Y., Zhou H. and Li S. (2022). BTN3A2 expression is connected with favorable prognosis and high infiltrating immune in lung adenocarcinoma. Front. Genet. 13, 848476.

Liu H. and Luo J. (2019). MiR-211-5p contributes to chondrocyte differentiation by suppressing Fibulin-4 expression to play a role in osteoarthritis. J. Biochem. 166, 495-502.

Liu M., Jin F., Yao X. and Zhu Z. (2022). Disease burden of osteoarthritis of the knee and hip due to a high body mass index in china and the USA: 1990-2019 findings from the global burden of disease study 2019. BMC Musculoskelet Disord. 23, 63.

Lively S., Moxon-Emre I. and Schlichter L.C. (2011). SC1/hevin and reactive gliosis after transient ischemic stroke in young and aged rats. J. Neuropathol. Exp. Neurol. 70, 913-929.

Ma Y., Xu Y. and Li L. (2018). SPARCL1 suppresses the proliferation and migration of human ovarian cancer cells via the MEK/ERK signaling. Exp. Ther. Med. 16, 3195-3201.

Mao H., Wang L., Xiong Y., Jiang G. and Liu X. (2022). Fucoxanthin attenuates oxidative damage by activating the Sirt1/Nrf2/HO-1 signaling pathway to protect the kidney from ischemia-reperfusion injury. Oxid. Med. Cell. Longev. 2022, 7444430.

Othumpangat S. and Noti J.D. (2023). β-defensin-1 regulates influenza virus infection in human bronchial epithelial cells through the STAT3 signaling pathway. Pathogens 12, 123.

Qiu Z., Ma X., Xie J., Liu Z., Zhang Y. and Xia C. (2021). MiR-1307-5p regulates proliferation and apoptosis of chondrocytes in osteoarthritis by specifically inhibiting transforming growth factor beta-induced gene. Am. J. Transl. Res. 13, 7756-7766.

Sieker J.T., Proffen B.L., Waller K.A., Chin K.E., Karamchedu N.P., Akelman M.R., Perrone G.S., Kiapour A.M., Konrad J., Murray M.M. and Fleming B.C. (2018). Transcriptional profiling of articular cartilage in a porcine model of early post-traumatic osteoarthritis. J. Orthop. Res. 36, 318-329.

Sui C., Zhang L. and Hu Y. (2019). MicroRNA let 7a inhibition inhibits LPS induced inflammatory injury of chondrocytes by targeting IL6R. Mol. Med. Rep. 20, 2633-2640.

Swingler T.E., Niu L., Smith P., Paddy P., Le L., Barter M.J., Young D.A. and Clark I.M. (2019). The function of microRNAs in cartilage and osteoarthritis. Clin. Exp. Rheumatol. 37 (Suppl. 120), 40-47.

Thomson A. and Hilkens C.M.U. (2021). Synovial macrophages in osteoarthritis: The key to understanding pathogenesis? Front. Immunol. 12, 678757.

Wang T. and He C. (2018). Pro-inflammatory cytokines: The link between obesity and osteoarthritis. Cytokine Growth Factor Rev. 44, 38-50.

Wang X., Fan J., Ding X., Sun Y., Cui Z. and Liu W. (2019). Tanshinone I inhibits IL-1β-induced apoptosis, inflammation and extracellular matrix degradation in chondrocytes CHON-001 cells and attenuates murine osteoarthritis. Drug. Des. Devel. Ther. 13, 3559-3568.

Wang Y., Shen S., Li Z., Li W. and Weng X. (2020). MIR-140-5p affects chondrocyte proliferation, apoptosis, and inflammation by targeting HMGB1 in osteoarthritis. Inflamm. Res. 69, 63-73.

Weng K., Luo M. and Dong D. (2020). Elucidation of the mechanism by which a ADAMTS5 gene microRNA-binding site single nucleotide polymorphism affects the risk of osteoarthritis. Genet. Test. Mol. Biomarkers 24, 467-477.

Xiao M., Hu Z.H., Jiang H.H., Fang W. and Long X. (2021). Role of osteoclast differentiation in the occurrence of osteoarthritis of temporomandibular joint. Hua Xi Kou Qiang Yi Xue Za Zhi. 39, 398-404.

Zhang H.P., Wu J., Liu Z.F., Gao J.W. and Li S.Y. (2022). SPARCL1 is a novel prognostic biomarker and correlates with tumor microenvironment in colorectal cancer. Biomed. Res. Int. 2022, 1398268.

Zhang S., Zhang F. and Feng L. (2021). The inhibition of HeLa cells

proliferation through SPARCL1 mediated by SPP1. Cytotechnology 73, 71-78.

Zheng T., Kang M.J., Crothers K., Zhu Z., Liu W., Lee C.G., Rabach L.A., Chapman H.A., Homer R.J., Aldous D., De Sanctis G.T., Underwood S., Graupe M., Flavell R.A., Schmidt J.A. and Elias J.A. (2005). Role of cathepsin S-dependent epithelial cell apoptosis in IFN-gamma-induced alveolar remodeling and pulmonary emphysema. J. Immunol. 174, 8106-8115.

Zhou F., Mei J., Han X., Li H., Yang S., Wang M., Chu L., Qiao H. and Tang T. (2019). Kinsenoside attenuates osteoarthritis by repolarizing macrophages through inactivating NF-κB/MAPK signaling and protecting chondrocytes. Acta Pharm. Sin. B. 9, 973-985.

Zhou C., He T. and Chen L. (2021). LncRNA CASC19 accelerates chondrocytes apoptosis and proinflammatory cytokine production to exacerbate osteoarthritis development through regulating the miR-152-3p/DDX6 axis. J. Orthop. Surg. Res. 16, 399.

Accepted July 26, 2023